ELSEVIER

Solar Energy Materials & Solar Cells 57 (1999) 277–290

Solar Energy Materials & Solar Cells

The effect of emitter recombination on the effective lifetime of silicon wafers

Andrés Cuevas*

Department of Engineering, FEIT, Australian National University, Canberra, ACT 0200, Australia

Received 4 June 1998; accepted 28 August 1998

Abstract

The application of photoconductance measurements of the effective lifetime of silicon wafers to determine the saturation current density of diffused emitter regions is reviewed. To illustrate the technique, a sequence of experiments is presented with phosphorus diffusions of various types: oxide passivated and unpassivated, lightly doped and heavily doped. Different material qualities (FZ, CZ and multicrystalline silicon) are considered, as well as different substrate resistivities. The dependence of the effective minority carrier lifetime on injection level is discussed. The limitations imposed by emitter recombination on the measurable minority carrier lifetimes are clarified and demonstrated experimentally. This bound varies with the dopant density and thickness of the silicon wafer.

Keywords: Lifetime; Photoconductance; Silicon

1. Introduction

Measurements of the minority carrier lifetime are becoming increasingly popular to characterise silicon wafers for photovoltaic applications. Besides relatively sophisticated techniques based on the transient decay of photoexcited carriers [1], simple instruments and methods [2] are contributing to make photoconductance techniques more widely available. In all cases, it is important to bear in mind that the measurable magnitude is a global recombination rate, that is, an effective minority carrier lifetime

* Fax: 61 2 62490506; e-mail: Andres.Cuevas@anu.edu.au

0927-0248/99/$ – See front matter
PII: S0927-0248(98)00179-2

that can be affected by several physical mechanisms simultaneously. The influence of the surface recombination velocity is well known and, in fact, measurements of τ_{eff} have been used to determine this important parameter for thermally grown SiO_2 [3] and also for plasma-deposited silicon nitride [4].

Diffused regions, that is, emitters, are omnipresent in solar cells, and they frequently dominate or have a strong effect on their overall performance. The measurement of τ_{eff} using a photoconductance instrument has also been proposed, and used, to determine the saturation current density that characterises the recombination in an emitter region [5]. As initially proposed, this determination relied on the use of high-resistivity silicon. The influence of J_o on the effective lifetime for the case of doped silicon (most commonly used for solar cells) has not been sufficiently explored. The present work intends to clarify this influence.

A sequence of experiments will lead the reader through a number of representative practical situations where the relative relevance of J_o and τ_{bulk} vary. To show different bulk minority carrier lifetimes, τ_{bulk}, we have selected a range of different materials, including FZ, CZ and multicrystalline silicon; furthermore, different dopant densities are used. To show the effect of different J_o the sheet resistance of the phosphorus diffusions and the surface passivation are modified. We commence with a succint description of the concept of the effective lifetime.

2. Components of the effective lifetime

Experimental evidence shows that the lifetime depends quite strongly on the carrier density level. To understand this dependence, let us evaluate the different recombination components known to be present in a silicon wafer, including bulk and surface contributions. The following theoretical analysis has been done with a steady-state situation in mind, but it is also representative of other experimental conditions. Appendix A summarises the steady-state method to determine the effective lifetime. Considering a sample of width W with a diffused region at each surface, the total recombination is given by the sum of the following terms:

$$\frac{1}{\tau_{\text{eff}}}\int_0^W \Delta n\,\mathrm{d}x = \frac{1}{\tau_{\text{bulk}}}\int_0^W \Delta n\,\mathrm{d}x + \frac{J_{o(\text{front})}}{qn_i^2}\Delta n(0)(\Delta n(0) + N_A) + \frac{J_{o(\text{rear})}}{qn_i^2}\Delta n(W)(\Delta n(W) + N_A). \quad (1)$$

The first term corresponds to bulk recombination, which can itself be dependent on the excess carrier density particularly, but not exclusively, in the transition between low and high injection levels. The minority carrier lifetime, τ_{bulk}, has been assumed to be independent of position, quite reasonable for a uniformly doped sample (high injection level and Auger recombination might compromise this in some situations). The second and third terms describe recombination at the diffused (emitter) regions by means of a saturation current density multiplied by the excess p–n product relative to

n_i^2 at the boundary of the corresponding space charge region. The position of this boundary has been defined as $x = 0$ for the front junction and $x = W$ for the rear junction. Note that recombination in the space charge region has been neglected in this simplified analysis, but it might be significant at very low injection levels. Obviously, the contribution of the rear surface will be negligible if the minority carrier diffusion length (due to τ_{bulk}) is lower than the wafer thickness. A similar expression can be written if a recombining interface exists at the surface, instead of a p–n junction. The surface recombination term is classically expressed as $S\,\Delta n\,(W)$, that is, the product of a surface recombination velocity and the excess carrier density. In low injection, an equivalence between surface recombination velocity and emitter saturation current can be established: $S_{eff} \approx J_o N_A / q n_i^2$.

In a similar way to the charge control model commonly used for the analysis of many electronic devices, all the different recombination mechanisms can be lumped together in a single parameter with time dimensions. The total recombination can, according to this interpretation, be expressed as the ratio of the minority carrier charge (the total number of minority carriers in the region under consideration) and an effective minority carrier lifetime. This is the meaning of the first member of Eq. (1). Defining an average excess carrier density

$$\Delta n_{av} = \frac{1}{W}\int_0^W \Delta n \, dx, \tag{2}$$

the effective lifetime can be obtained from Eq. (1):

$$\frac{1}{\tau_{eff}} = \frac{1}{\tau_{bulk}} + 2\,\frac{J_o}{q n_i^2 W}\,\frac{\Delta n(0)}{\Delta n_{av}}\,(\Delta n(0) + N_A). \tag{3}$$

To write the last expression, $\Delta n(0) \approx \Delta n(W)$ has been assumed together with identical front and back emitter regions, as applies to most of our experiments. This also means that $\Delta n(0) \approx \Delta n_{av}$, a reasonable simplification when the minority carrier diffusion length is higher than the wafer thickness. Care should be exercised when the excess carrier density is not uniform. In certain cases it is possible to account for the non-uniformity in a simple way; for example when $L \ll W$ and the spectrum of the illumination is rich in blue and violet colours (white light), $\Delta n(0) \approx \Delta n_{av} W/L$ is a better approximation. A non-uniform carrier density can also result if J_o is very high at the rear, the illumination is white and very strong and the sample is relatively thick. These special cases are discussed in Appendix B.

3. Wafers with lightly diffused surfaces

An assortment of silicon wafers including float zone, Czochralski and multicrystalline material of different resistivities was used in this experiment to cover a range of practical cases. Important details for these wafers, including dopant density and thickness, are given in Table 1. The first experiment was intended to reveal the

Table 1

Experimental measurements and expected limits to the measurable lifetime imposed by emitter recombination. Two cases are shown: a well passivated emitter ($J_{o(pass)} \approx 1.7 \times 10^{-14}$ A cm^{-2}) and the same emitter after the passivating oxide had been stripped ($J_{o(unpass)} \approx 1.5 \times 10^{-12}$ A cm^{-2}). The experimental τ_{eff} corresponds to its maximum value. The limit to τ_{eff} has been calculated as $qn_i^2W/(2J_oN_A)$. (*) The factor 2 has been dropped for samples F5 and M4 because $L \ll W$

Sample	ρ_b (Ω cm)	N_A (cm^{-3})	Thickness (μm)	τ_{eff} (passivated) (μs)	τ_{eff} $J_{o(pass)}$ limit (μs)	τ_{eff} (unpassiv.) (μs)	τ_{eff} $J_{o(unpass)}$ limit (μs)
F1	1000	1.4×10^{13}	256	**1200**			
F2	20	5×10^{14}	260	**830**	17000	**110**	192
F3	1.1	1.4×10^{16}	367	**400**	900	**8.5**	9.8
F4	0.46	3.6×10^{16}	290	**166**	280	**3.3**	3
F5	0.12	1.8×10^{17}	270	**10**	47	**1**	0.92(*)
CZ	0.59	2.7×10^{16}	253	**62**	290	**3.2**	3.5
M1	1.5	1×10^{16}	370	**20**	1280	**3.3**	14.5
M2	1.0	1.5×10^{16}	360	**15**	830	**3.3**	9.4
M3	0.42	4×10^{16}	350	**20**	300	Trapping	3.4
M4	0.2	1×10^{17}	345	**20**	120	**1.6**	2.4 (*)

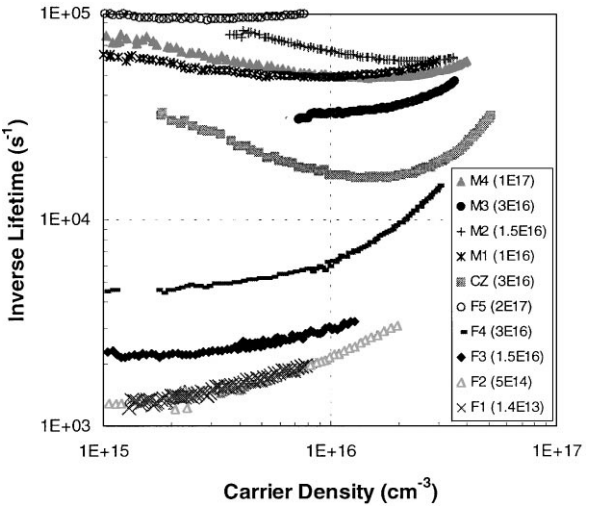

Fig. 1. Inverse effective lifetime as a function of carrier injection level for silicon wafers after a light phosphorus diffusion and oxide surface passivation. Samples F1 – F5 are float zone, M1 – M4 multicrystalline and CZ is Czochralski silicon.

electronic quality of the material, that is, the bulk minority carrier lifetime. For this, it is necessary to passivate the surfaces, and one of the most effective ways of doing so is to perform a light phosphorus diffusion followed by the growth of a silicon dioxide layer. Of course there are other methods of reducing surface recombination including the straight growth of a silicon dioxide layer. We have chosen a phosphorus diffusion in this experiment because it provides, in principle, a more stable surface boundary condition and is similar to the device structure of interest. The wafers were cleaned and subjected to a light phosphorus diffusion at 840°C, "in situ" oxide passivation at 900°C and forming gas annealed at 400°C; the sheet resistance of the n-type diffusion was 460 Ω.

The effective lifetime was measured using an induction coupling photoconductance instrument [6] and a photographic flash to achieve a wide range of carrier injection levels. Both the conventional transient photoconductance decay (PCD) and the quasi-steady-state (QSSPC) [2] methods were used to cover a broad range of effective lifetimes. The QSSPC method is almost essential when the bulk lifetime is very low or the emitter saturation current is very high.

Fig. 1 shows the inverse of the measured effective minority carrier lifetime as a function of the excess carrier density for the different wafers. These graphs visualise the overall recombination rate at a given carrier density. Vastly different minority carrier lifetimes, between 10 μs and 1.2 ms, are obtained in correspondence with the different material resistivities and growth techniques. The presence of a passivated light phosphorus diffusion exposes the bulk minority carrier lifetimes quite clearly although its possible influence cannot be completely ignored. In fact, the measured lifetimes can only be said to be a lower bound on the real τ_{bulk}. The maximum value of

the effective lifetime corresponds to the "valley" of the curves, and has been collected in Table 1 for each of them.

3.1. Determination of the emitter saturation current

A specific recombination parameter, τ_{bulk} or J_o for example, can only be determined accurately if the corresponding physical mechanism is dominant; it is difficult to determine τ_{bulk} if J_o is very high, and vice versa. The different dependence with injection level of the different recombination mechanisms provides an additional opportunity for their separation. At sufficiently high carrier densities the recombination in the emitter regions contains a term that is proportional to $(\Delta n)^2$. The Auger recombination mechanism is proportional to $(\Delta n)^3$ and can also be significant, particularly if very high injection levels are reached. Once the Auger term has been subtracted, the plot of $1/\tau_{eff}$ vs. Δn shows a constant slope that is attributable to recombination in the diffused regions only. This is described by the following expression:

$$\frac{1}{\tau_{eff}} = \frac{1}{\tau_{bulk}} + 2\frac{J_o}{qn_i^2 W}(N_A + \Delta n). \tag{4}$$

The effect of emitter recombination is usually noticeable already at excess carrier densities five or ten times lower than the dopant density. For a clean extraction of the saturation current density J_0 the sample must be well in high injection, a condition relatively difficult to reach in doped material. The use of a lowly doped sample that can easily be highly injected by the light excitation ($\Delta n \gg N_A$) facilitates the measurement. This method, proposed by Kane [5] in the context of the transient photoconductance decay technique, can also be used with a quasi-steady-state approach. Applying it to the two FZ wafers in Fig. 1 with resistivities higher than 20 Ωcm we obtain $J_o \approx 1.7 \times 10^{-14}$ A cm^{-2} per side at 25°C. This very low saturation current density is representative of the lowly doped, surface passivated phosphorus emitter present in these wafers.

3.2. Limitation on the bulk minority carrier lifetime

The possibility of obtaining the bulk lifetime from an extrapolation of the $1/\tau_{eff}$ vs. Δn plot to the $\Delta n = 0$ axis, also proposed in Ref. [5], is not generally valid. An exception is the case of lowly doped samples with a relatively low J_o typically considered in Ref. [5] and similar studies. Mathematically, τ_{bulk} could be obtained extrapolating the linear part of the $1/\tau$ vs. Δn curve to $\Delta n = -N_A$ (see Eq. (4)). In actual fact, the maximum value of τ_{eff} that can be measured at very low carrier density levels is

$$\left.\frac{1}{\tau_{eff}}\right|_{min} = \frac{1}{\tau_{bulk}} + 2\frac{J_o}{qn_i^2 W} N_A. \tag{5}$$

It is interesting to note that a given J_o produces a different limitation to the measurable lifetime depending on the resistivity of the wafer, with the higher doping densities placing a more stringent limit. The experimental results shown in Fig. 1 provide a good evidence of this limitation. The highest effective lifetimes measured for the different wafers are compared in Table 1 with the corresponding limit imposed by the saturation current density. For the calculations we have used $qn_i^2 = 11.75\ \mathrm{C\ cm^{-6}}$ (at 25°C) and $J_o \approx 1.7 \times 10^{-14}\ \mathrm{A\ cm^{-2}}$, as obtained from the high injection measurements of samples F1, and F2. This saturation current density is so low that it does not pose a real problem for most samples in this experiment. Wafers F3 and F4 are an exception, because the expected contribution due to J_o is of the same order as the measured τ_{eff}. The real τ_{bulk} for these two wafers can exceed considerably the measured τ_{eff}; a simple evaluation based on Eq. (5) would give τ_{bulk} up to 750 and 500 μs, for F3 and F4, respectively. A still better passivation would be required to measure τ_{bulk} directly in these wafers.

Thanks to the inclusion of a high-resistivity sample and the subsequent determination of J_o, it has been possible to verify that the measured τ_{eff} of the lower quality wafers, including the CZ sample and the multicrystalline wafers, can be interpreted to be a true reflection of τ_{bulk}. This conclusion cannot be reached "a priori".

In principle, the $1/\tau_{eff}$ vs. Δn curves should follow a straight line down to zero excess carrier densities, as predicted by Eq. (4). The experimental evidence is that the curves tend to saturate or even go upwards at very low carrier densities. The actual bulk lifetime at low injection levels is usually significantly lower than what the extrapolation of the $1/\tau_{eff}$ vs. Δn curves would indicate. This can be explained by the fact that recombination in the bulk also depends on Δn, according to the traditional Shockley–Read–Hall formulation [7]; that is, τ_{bulk} is not constant. In addition, recombination in the depletion region of the p–n junction can become significant at very low carrier density levels.

3.3. Unpassivated diffused regions

To further illustrate the point made in the previous section, the influence of emitter recombination was exacerbated by stripping the passivating oxide in hydrofluoric acid. The measurements corresponding to the same samples after oxide removal are shown in Fig. 2. The unpassivated emitters present a very high J_o, as is apparent in the more pronounced slope of the curves. From this slope $J_o \approx 1.5 \times 10^{-12}\ \mathrm{A\ cm^{-2}}$, approximately two orders of magnitude higher than for the passivated case. The two surface conditions are compared in Fig. 3 for the 20 Ωcm wafer. Note that both curves converge at $\Delta n \approx -N_A$, as predicted by Eq. (4). It is obvious that the accuracy of the extrapolation to determine the bulk lifetime is quite poor when J_o is very high.

The maximum detectable lifetime is now much lower for all the samples, as predicted by Eq. (5). Table 1 contains a summary of the measured τ_{eff} together with theoretical calculations of the limit imposed by J_o. This bound is very restrictive for the lower resistivity wafers; for example, τ_{eff} of F3 ($N_A = 1.5 \times 10^{16}\ \mathrm{cm^{-3}}$) has decreased from 400 to 8.5 μs after removing the passivating oxide from the diffused

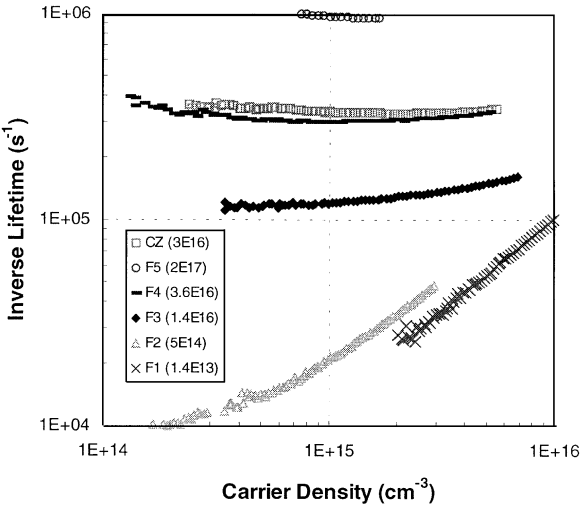

Fig. 2. Inverse effective lifetime as a function of carrier injection level for the case of an unpassivated light phosphorus diffusion.

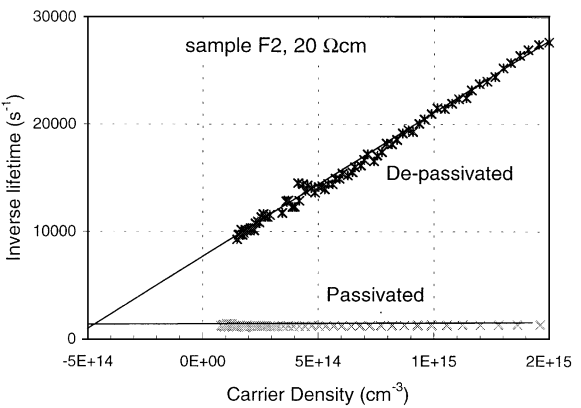

Fig. 3. Effect of stripping the passivating oxide from the surface of a light phosphorus diffusion. The extrapolations of the two curves intersect at $\Delta n \approx -N_A$.

surfaces. τ_{eff} of F4 ($N_A = 4 \times 10^{16}$ cm^{-3}) has decreased from 166 to 3.3 μs; the other samples have also suffered drastic reductions. The bound on τ_{eff} imposed by the very high J_o explains quite well the measured lifetimes in most cases. This provides further evidence of the validity of Eq. (5) and stresses the importance of good surface passivation to unveil the bulk lifetime. In fact, the effective lifetimes measured for the case of a very high J_o are similar in magnitude to the case of an infinite surface recombination velocity. Note that a $J_o \approx 1.5 \times 10^{-12}$ A cm^{-2} can be translated into an equivalent surface recombination velocity $S_{eff} \approx J_o N_A / q n_i^2 \approx 2 \times 10^4$ cm s for sample F3 (1 Ω cm).

An alternative method to determine J_o in cases where it is clearly dominant over bulk recombination is to identify the measured effective lifetime at low carrier densities with the J_o term in Eq. (5). The agreement between the calculated and experimental values for the case of unpassivated emitters constitutes a good example of this possibility. We shall use it in the next section.

4. The case of a heavily phosphorus doped region

Industrial solar cells typically have a relatively heavily doped region as emitter region. The sheet resistance is quite low, around 40 Ω, to accommodate for the needs of the screen printed metallisation commonly used. Recombination in such a diffused region is relatively high, and it generally is a limiting factor for commercial solar cells. Another relevant case where heavy phosphorus diffusions are used is to getter unwanted impurities from the material. This is particularly important for cast multicrystalline silicon, where the levels of contamination are quite high in the top and tail regions of the ingots.

In our series of experiments, the same silicon wafers were etched to eliminate the previous lightly diffused regions and then subjected to a phosphorus gettering treatment for 3 h. The heavy phosphorus diffused layer had a sheet resistance of 10 Ω and produced a severe limitation on the measurable effective lifetimes. This is a situation commonly found in industrial solar cells, where the actual quality of the material can be obscured, at least partly, by the contribution of the emitter region (and sometimes also the rear surface).

Although we could determine the saturation current density J_0 corresponding to this heavy diffusion using a high-resistivity wafer we will follow the alternative procedure mentioned in the previous section. We can attribute the measured $\tau_{eff} = 33$ μs in the 1 Ω cm F3 wafer to emitter recombination only, since we know that the bulk lifetime is much higher (at least $\tau_{eff} = 400$ μs measured with a light diffusion, possibly $\tau_{bulk} = 750$ μs). The saturation current density J_o can then be evaluated from $1/\tau_{eff} = 2J_oN_A/qn_i^2W$. The result, $J_o \approx 4 \times 10^{-13}$ A cm^{-2} per side, is intermediate between the passivated and unpassivated light diffusion cases presented above. This value of J_o can now be used to evaluate the limit that it imposes on τ_{eff} for the remaining wafers in the experiment. Fig. 4 shows an excellent agreement between this limit and the measured lifetimes for most of the samples. The results are also collected in Table 2.

As evidenced by the experimental results, even if emitter recombination is the dominant mechanism, samples with identical diffusions can show different effective lifetimes if they have a different dopant density or a different thickness. An additional experiment illustrated this point in a curious manner: after a heavy phosphorus diffusion we found that a 1.5 Ω cm multicrystalline silicon sample had an effective lifetime of 22 μs, while a control 1 Ω cm FZ wafer had a lower $\tau_{eff} = 13$ μs. This surprising result was eventually understood after realising that the emitter recombination was dominant ($J_o \approx 7.2 \times 10^{-13}$ A cm^{-2}), considering the doping (1.5 times) and thickness (400 μm and 240 μm, respectively) differences between the wafers.

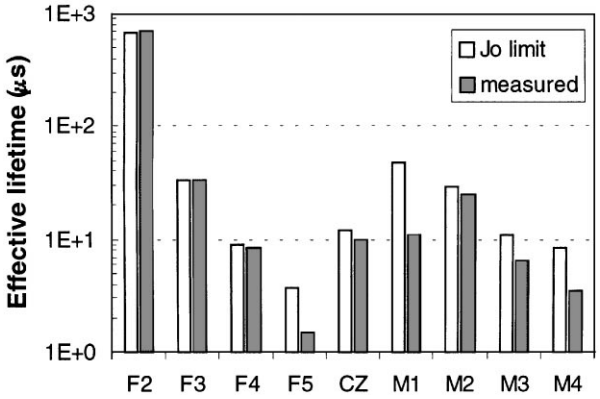

Fig. 4. Comparison between the measured effective lifetime after a heavy, 10 Ω phosphorus diffusion and the limit imposed by the emitter recombination current.

Table 2
Experimental measurements and expected limits to the measurable lifetime for the case of a heavy phosphorus diffusion ($J_o \approx 4 \times 10^{-13}$ A cm^{-2}). The final lifetime after the gettering treatment is also given. The most likely value of the bulk minority carrier diffusion length after gettering (obtained after subtracting an emitter contribution $J_o \approx 3 \times 10^{-14}$ Acm^{-2} from $\tau_{eff(gett)}$, is given in the last coloum

Sample	N_A (cm^{-3})	Thickness (μm)	$\tau_{eff(meas.)}$ (heavy n$^+$) (μs)	τ_{eff} ($J_{o(n+)}$ limit) (μs)	$\tau_{eff\ (meas.)}$ (gettered) (μs)	L_{bulk} (μm)
F1	1.4×10^{13}	240			**4000**	3900
F2	5×10^{14}	234	**700**	670	**1600**	2600
F3	1.4×10^{16}	334	**33**	33	**350**	2100
F4	3.6×10^{16}	234	**8.5**	9	**80**	750
F5	1.8×10^{17}	237	**1.5**	3.7	**7.5**	120
CZ	2.7×10^{16}	227	**10**	12	**75**	600
M1	1×10^{16}	345	**11**	48	**48**	385
M2	1.5×10^{16}	310	**25**	29	**200**	1000
M3	4×10^{16}	315	**6.5**	11	**40**	350
M4	1×10^{17}	300	**3.5**	8.5	**18**	190

5. Effect of phosphorus gettering

Subsequently, the heavy phosphorus diffusion was removed (about 10–15 μm of silicon were etched) and a new light diffusion was performed in the same conditions as the initial diffusion. The resulting sheet resistance of this passivated diffusion was 450 Ω, nearly the same as the initial pre-gettering diffusion, although its saturation current was slightly higher ($J_o \approx 3 \times 10^{-14}$ Acm^{-2} per side). Fig. 5 shows the inverse of the measured effective minority carrier lifetime as a function of the excess carrier density for the different wafers. The beneficial effect of the gettering treatment on the mc-Si wafers is remarkable, although it is not equally important for all wafers. Sample

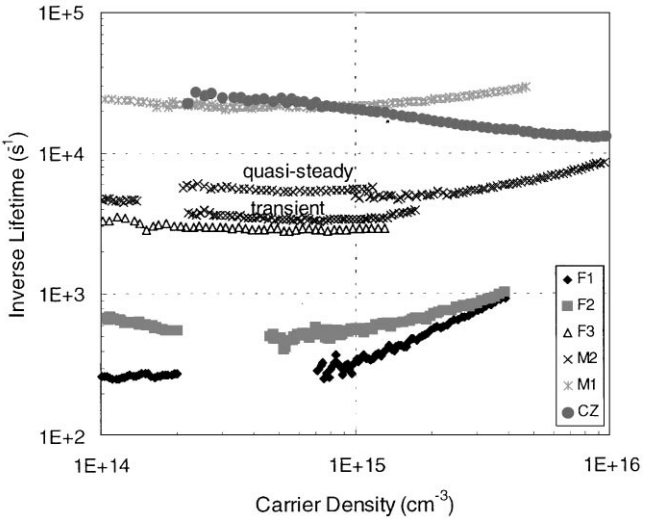

Fig. 5. Effective lifetime after a gettering treatment. Both QSSPC and transient PCD measurements are included.

M4, 0.2 Ω cm, remained essentially unchanged. Samples M1 and M2 have almost the same resistivity, 1.5 Ω cm, although they come from different ingots; notably, the resistivity of M1 was obtained with a compensation factor of 1.5. The lifetime of M2 increased with gettering by a factor of 10, while that of M1 doubled. In Fig. 5 both transient PCD and QSSPC measurements of M2 are included; the transient measurement is slightly optimistic for this material. The efficacy of the gettering treatment seems to be highest for wafers that had a stronger variation of the lifetime at very low injection levels before gettering. This also applies to the CZ wafer.

The gettering step has also improved τ_{bulk} in the higher resistivity FZ wafers. Very low injection measurements (included in Fig. 5) indicate lifetimes of 4 ms for F1 and 1.6 ms for F2. Note that the extrapolation of the curves to zero carrier density would be optimistic. The lower resistivity FZ wafers seem, however, affected by the J_o of this diffusion, since their lifetimes after gettering (given in Table 2) are slightly lower than before gettering (see Table 1), which had a better surface diffusion. After subtracting the emitter contribution from τ_{eff} to obtain τ_{bulk} the likely values of the minority carrier diffusion length in the bulk of the semiconductor after gettering can be estimated (last column of Table 2).

6. Conclusions

Photoconductance measurements are a convenient technique to study the various recombination mechanisms that coexist in a semiconductor and the corresponding

characteristic parameters, in particular bulk minority carrier lifetime, surface recombination velocity and emitter saturation current. To discriminate between them a careful physical interpretation of the experimental data is necessary. The most significant findings of this work are summarised below.

The effective lifetime is always susceptible to vary with injection level. The extent of this variation is different for every sample. Some general trends can, nevertheless, be identified in the experimental measurements. Usually the effective lifetime increases with injection level at very low carrier density levels, reaches a maximum and then decreases at high injection levels. Given that, in the experimental situation presented here, the surfaces are bound by a p–n junction that establishes a constant boundary condition at low injection levels (no injection dependence), the variation at low injection levels can be attributed to changes of the bulk minority carrier lifetime. The latter can be explained in terms of the Shockley-Read-Hall model for recombination via flaws.

Diffused regions can help to reduce the overall surface recombination. Even so, they set an upper bound on the measurable lifetime given by $qn_i^2W/2J_oN_A$. This bound can be very restrictive for highly doped and for thin wafers. It is particularly stringent if the saturation current density of the emitter region is very high. For example an unpassivated light phosphorus diffusion can limit τ_{eff} to only 9 μs in 1 Ω cm wafers. In such extreme cases the measured effective lifetime can be used to determine the saturation current density J_o.

Recombination in emitter regions becomes even more important as the carrier density becomes higher than one-tenth of the wafer doping, approximately. A measurement of the photoconductance as a function of light intensity permits to determine the emitter saturation current. The determination of J_o is facilitated by the use of high-lifetime, high-resistivity wafers to ensure that the measured effective lifetime is clearly dominated by the emitter regions.

The maximum effective lifetime occurs at an injection level that results from a trade-off between the mechanisms mentioned above. The particular injection level at which this happens differs from sample to sample, although it typically lies in the vicinity of the wafer dopant density.

Acknowledgements

The Australian Research Council has provided support for this work. Thanks to Chris Samundsett for sample preparation.

Appendix A. The quasi-steady-state photoconductance method

The measurement of the photoconductance of a semiconductor sample under steady (or quasi-steady)-state illumination, together with a measurement of the photogeneration rate can be used to determine the effective minority carrier lifetime,

τ_{eff}, according to the following expressions:

$$J_{\text{ph}} = \frac{q\int_0^W \Delta n \, \mathrm{d}x}{\tau_{\text{eff}}} = \frac{q\Delta n_{\text{av}} W}{\tau_{\text{eff}}}, \tag{A.1}$$

$$\sigma_L = q\int_0^W (\Delta n\mu_{\text{n}} + \Delta p\mu_{\text{p}}) \, \mathrm{d}x \approx q\Delta n_{\text{av}}(\mu_{\text{n}} + \mu_{\text{p}})W, \tag{A.2}$$

$$\tau_{\text{eff}} = \frac{\sigma_L}{J_{\text{ph}}(\mu_{\text{n}} + \mu_{\text{p}})}. \tag{A.3}$$

Eq. (A.1) is a statement of the balance between generation (expressed as J_{ph}/q) and recombination, where the latter is given by the total number of excess minority carriers divided by the effective lifetime, while Eq. (A.2) gives the increase in conductance produced by the photogenerated carriers. The conductance and the incident light intensity can be measured using a calibrated instrument and a reference solar cell, respectively. For a given irradiance, the total photogeneration within the sample J_{ph} can be easily estimated. The electron and hole mobilities of silicon are well known.

In general, the excess carrier density is position dependent; the average carrier density, Δn_{av}, has been used in Eq. (A.1) and (A.2). Eq. (A.2) also assumes that the electron and hole mobilities are approximately constant across the sample and their possible carrier density dependence is accommodated for by evaluating them at the average carrier concentration. Eq. (A.2) should be iterated to find a self consistent set of values for both Δn_{av} and $(\mu_{\text{n}} + \mu_{\text{p}})$, although this iteration is not necessary if the sample is in low injection.

Appendix B. Additional considerations for the determination of J_{o}

The assumption of a uniform excess carrier density can fail in certain cases, for example when the diffusion length is smaller than the wafer thickness $L \ll W$. In that case, assuming that most of the light is absorbed near the surface (white or blue-rich illumination), a better approximation is $\Delta n(0) \approx \Delta n_{\text{av}} W/L$. In such a case, the plot of $1/\tau_{\text{eff}}$ vs. Δn_{av} will show a greater slope and the standard analysis would yield $J_{\text{o}}W/L$, rather than $2J_{\text{o}}$. Note that at very high injection levels Auger recombination could make $L < W$ in certain cases, and this would exacerbate the apparent slope of the $1/\tau_{\text{eff}}$ vs. Δn_{av} curve.

A non-uniform carrier density also happens if $J_{\text{o(rear)}}$ (or equivalently, the surface recombination velocity) is very high at the rear surface. A possible situation would be that the bulk minority carrier lifetime is high, $L \gg W$, and the rear recombination rate is very high, making $\Delta n(W) \approx 0$. The carrier density profile would be approximately a straight line and $\Delta n(0) \approx 2\Delta n_{\text{av}}$. The slope of the $1/\tau_{\text{eff}}$ vs. Δn_{av} curve would, in theory, give $4J_{\text{o(front)}}$, although the effective lifetime would likely be quite low and dominated by the high recombination rate at the rear surface.

For high injection levels and high J_{o} an additional consideration should be made. If the source of light is white most of the excess carriers are generated near the front

surface. Part of these carriers will travel to the rear of the wafer to recombine in the second emitter region present there. This diffusion of carriers necessitates that a gradient in the excess carrier density profile is formed. The gradient, that is, the current to be transported to the rear, can be quite large if $J_{o\ rear}$ is high, especially when the illumination intensity is also high. Although an accurate description of the carrier density profile requires computer simulations, it is possible to reflect the inequality between $\Delta n(0)$ and $\Delta n(W)$ in the expression for $1/\tau_{eff}$ in an approximate way if a linear profile is assumed (bulk recombination negligible). The average carrier density is then $\Delta n_{av} \approx [\Delta n(0) + \Delta n(W)]/2$. Considering equal front and rear J_o,

$$\frac{1}{\tau_{eff}} = \frac{J_o}{qn_i^2 W} \frac{2(\Delta n(0)^2 + \Delta n(W)^2)}{\Delta n(0) + \Delta n(W)}. \tag{B.1}$$

In addition, the gradient can be evaluated by realising that the diffusion current towards the rear should equal the recombination at the back junction

$$D_{amb} \frac{\Delta n(0) - \Delta n(W)}{W} \approx \frac{J_o}{qn_i^2} \Delta n(W)^2. \tag{B.2}$$

A third relationship needed to solve for J_o is provided by the measured photoconductance (see Appendix A). Note that, in high injection, an ambipolar diffusion coefficient should be used $D_{amb} \approx 18\ cm^2/s$ [8].

A possible way to reduce uncertainties in the analysis that can result from a non-uniform carrier density profile is to use infrared light. Weakly absorbed light produces more symmetric conditions at both surfaces and a more uniform carrier density profile, except for extremely high surface or emitter recombination.

References

[1] A. Schönecker, K. Heasman, J.Schmidt, J. Poortmans, T. Bruton, W. Koch, Results of five solar silicon wafer minority carrier lifetime round robins organised by the SEMI M6 solar silicon standardisation task force, Proc. 14th European Photovoltaic Solar Energy Conf., Barcelona, 1997, pp. 666–671.
[2] R.A. Sinton, A. Cuevas, Appl. Phys. Lett. 69 (17) (1996) 2510.
[3] F.M. Schuurmans, J. Schmidt, W. Sinke, A. Aberle, A comparative study between light-biased MW-PCD and MFCA measurements on high quality surface passivated silicon wafers, Proc. 14th European Photovoltaic Solar Energy Conf., Barcelona, 1997, pp. 1361–1364.
[4] T. Lauinger, J. Schmidt, A. Aberle, R. Hezel, Appl. Phys. Lett. 68 (1996) 1232.
[5] D.E. Kane, R.M. Swanson, Measurement of the emitter saturation current by a contactless photoconductivity decay method, Proc. 18th IEEE Photovoltaics Specialist Conf., Las Vegas, 1985, IEEE, New York, 1985, p. 578.
[6] Sinton Consulting, 1132 Green Circle, Boulder, CO 80303.
[7] J.S. Blakemore, Semiconductor Statistics, International Series of Monographs on Semiconductors, vol. 3, Pergamon Press, Oxford, 1962.
[8] D.E. Kane, R.M. Swanson, Effect of electron-hole scattering on the current flow in semiconductors, J. Appl. Phys. 72 (1992) 5294.